

Modelling of Mechanical Loads on Thin Film Solar Cell Structures

Norbert Schwarzer, Saxonian Institute of Surface Mechanics, Lieschow 26, 18569 Ummanz, Germany, n.schwarzer@siomec.de; www.siomec.de

Abstract

Within this short note a variety of loading situations on thin film solar cell structures is investigated in order to find worst case contact situations, study the effect of impact and detect mechanically weak points in the multi-layer structure such a device is usually made of. The effect of intrinsic stresses and defects is mentioned and an example is investigated but it will be considered in more detail in a second study.

Introduction

There are quite a number of methods to estimate the life time and efficiency-development of solar cells, be it for rather monolithic or thin film (multi-layer) structure. A very often neglected point within almost all of these models however, is the mechanical loading of the solar cells during their production, installation and service life. There usually is no question about the need of knowing the mechanical load limits of such structures for the purpose of production, transport and installation, but rather often people ask why this topic is also interesting after the installation when, the solar cell apparently rests safe and peacefully on a roof, a wall, within a window or on a secured ground area. Here it obviously is difficult to make the user understand what disastrous effects rain drops, hailstones or even dust particles can have, if they hit the solar cell structure with sufficient force. Not to mention flying bigger objects in stormy weather, insects, bird drops or the wrong method of cleaning. Even though most thin solar structures are often covered with additional layers of glass it might be useful to know its load limits. This is not only interesting because the glass protection might not always be there (in order to avoid additional energy loss), but also because concentrated contact forces on the underlying thin film cell can be caused by the glass-plate's natural roughness and interlaying particles (dust). For the determination of the maximum roughness and acceptable dust concentration alone, the modelling demonstrated here might be useful. It is also often forgotten, that the natural inner structure of thin film solar cells itself lead to concentrated mechanical loads in the case of external excitation. So even without direct mechanical contact caused by dust or other "alien elements" the thin film solar cell is subjected to such concentrated mechanical loads triggered by unavoidable influences like, wind pressure, permanent environmental oscillations, thermally induced and atomic mismatch stresses. As mathematically however, it makes no difference whether these loads are modelled as internally or externally triggered loads, we will concentrate here on external contact ones. Thus, the reader should bear in mind, that the resulting limiting stress fields presented for such loading situations are also applicable (without much altering) in the case of internally induced fields, caused by macro particles, columnar or grain structures or other imperfect interfaces for instance. As by summing up all mechanical loads the estimated mechanically induced degradation reaches an amount of over 50% of the whole it might be interesting and worthwhile to consider this wide variety of reasons of failure more closely.

Examples

As an example we pick a relatively simple thin film solar cell structure from the literature [1] and subject it to a variety of mechanical loading situations in order to study their effects. Therefore we at first define the multi-layer structure as shown in fig. 2a within the software package FilmDoctor (fig. 1 and [2 - 8]).

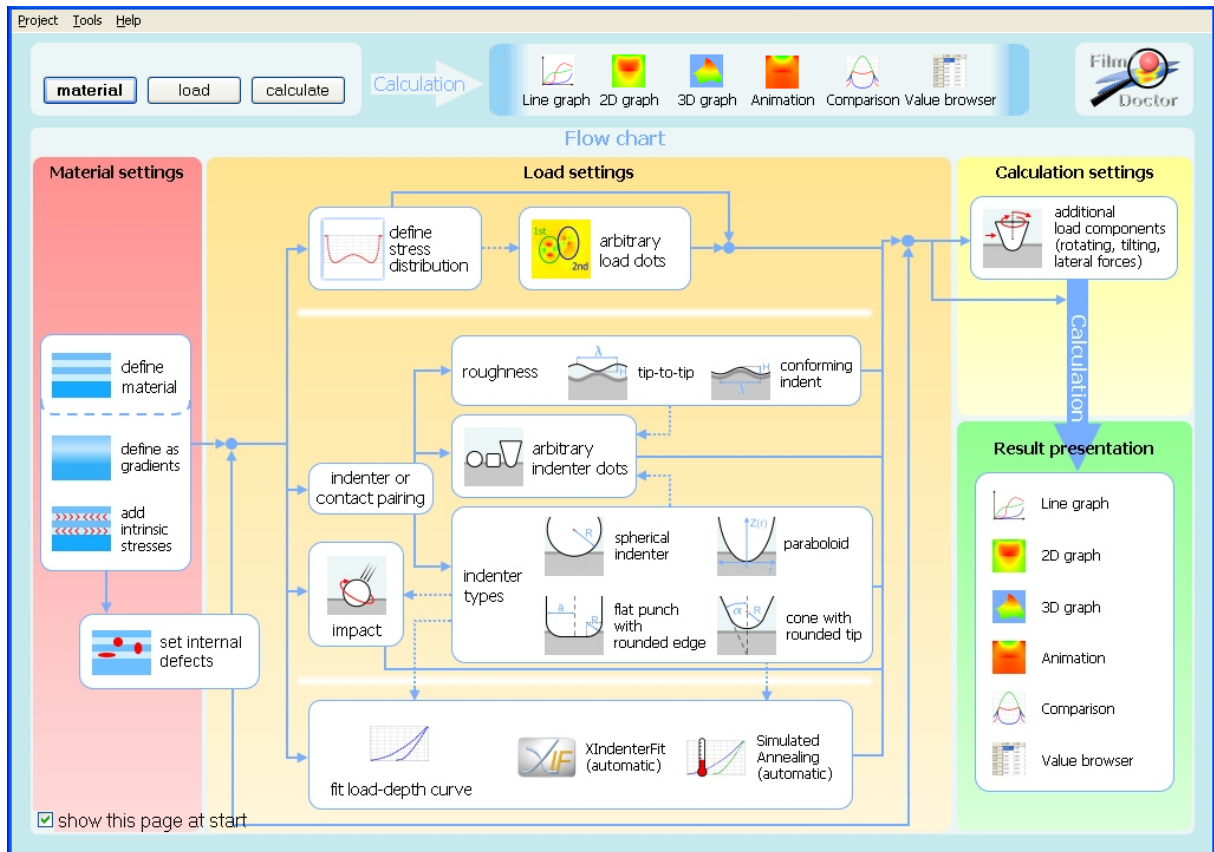


Fig. 1: Simulating mechanical loading in three steps: Material definition, load setting, evaluation → view.

Simulating roughness and dust “scratching”

The next step is choosing a suitable loading method (fig. 2b). For the reason of simplicity we here start with a spherical diamond indenter of 50 μm radius (fig. 3 red rectangle), because this type of indenters is widely used in nanoindentation for the purpose of investigating thin film structures. The size if the radius of curvature of the indenter is chosen such, that it might also simulate a dust particle or an contacting asperity from the protective glass cover for instance.

step 1: select your material use internal defects

	Poisson's ratio	Young's modulus	select from database	layer thickness	intrinsic stresses		
	<input type="checkbox"/> gradient				<input type="checkbox"/> gradient	<input type="checkbox"/> gradient	
<input type="checkbox"/> layer 1: ν : 0,235	E: 66	GPa	Glass AF 45 (Schott) (E:1	h: 3000	μm	in x: 0	GPa in y: 0 GPa
<input checked="" type="checkbox"/> layer 2: ν : 0,35	E: 105	GPa	ZnO-n (E:)	h: 0,7	μm	in x: 0	GPa in y: 0 GPa
<input checked="" type="checkbox"/> layer 3: ν : 0,35	E: 110	GPa	ZnO-i (E:110)	h: 0,05	μm	in x: 0	GPa in y: 0 GPa
<input checked="" type="checkbox"/> layer 4: ν : 0,37	E: 40	GPa	user defined	h: 0,02	μm	in x: 0	GPa in y: 0 GPa
<input checked="" type="checkbox"/> layer 5: ν : 0,25	E: 40	GPa	Absorber TF-Solar CuG	h: 1,5	μm	in x: 0	GPa in y: 0 GPa
<input checked="" type="checkbox"/> layer 6: ν : 0,38	E: 329,9	GPa	Molybdenum (Mo) (E:32	h: 0,1	μm	in x: 0	GPa in y: 0 GPa
<input type="checkbox"/> layer 7: ν : 0,208	E: 82	GPa		h: 5	μm	in x: 0	GPa in y: 0 GPa
<input type="checkbox"/> layer 8: ν : 0,208	E: 82	GPa		h: 5	μm	in x: 0	GPa in y: 0 GPa
<input type="checkbox"/> layer 9: ν : 0,208	E: 82	GPa		h: 5	μm	in x: 0	GPa in y: 0 GPa
<input type="checkbox"/> layer 10: ν : 0,208	E: 82	GPa		h: 5	μm	in x: 0	GPa in y: 0 GPa
substrate: ν : 0,206	E: 82	GPa	Glass N-BAK4 (Schott) (l		μm	in x: 0	GPa in y: 0 GPa

Fig. 2a: Material definition page. Material parameters from the SIO data-bank or [1].

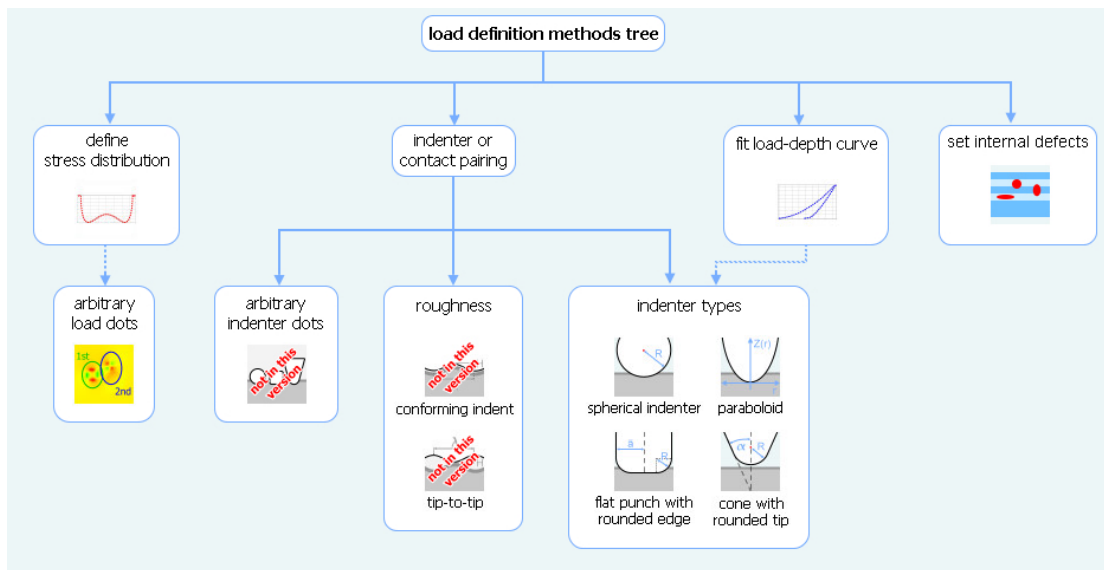


Fig. 2b: Choosing “spherical indenter” from the load definition methods tree.

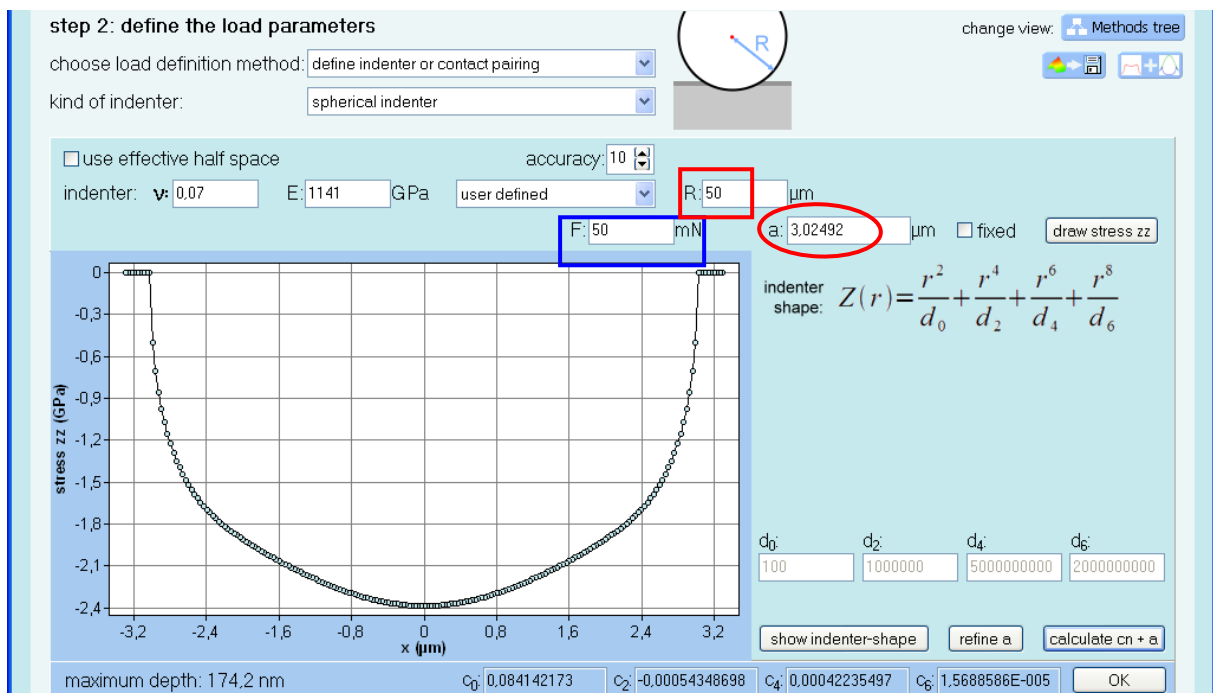


Fig. 3: Evaluation of the contact load (radius and normal stress distribution) of a spherical diamond indenter.

We apply a rather moderate load of 50mN (blue rectangle) and find the resulting contact radius of $a=3.02\mu\text{m}$ (red ellipse) and a rather non-Hertzian surface stress distribution shown in the diagram in fig. 3. By pressing the OK-button we directly come to the calculation page and define the area for which we intend to evaluate the stress field.

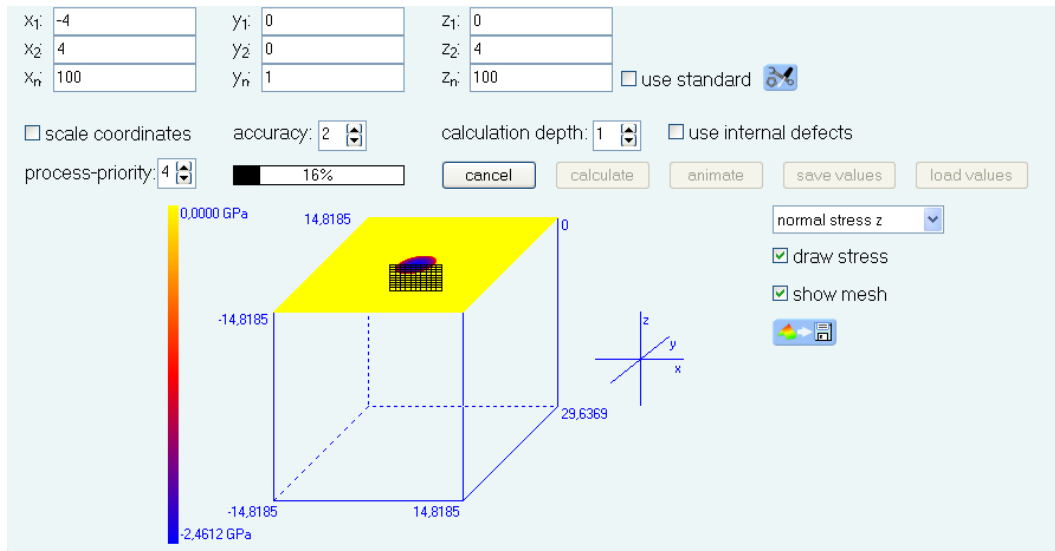


Fig. 4: Calculation-page: Setting the range of calculation of the complete elastic field.

Then the evaluation can be started by pressing “calculate”(fig. 4) and after only a few seconds the complete contact field with 280000 components is evaluated and ready to be investigated by the means of line-diagrams, 2D contour-plots and 3D-graphs.

Here we restrict ourselves to explore the field with the 2D-graph feature. From the view selector we select the important von Mises stress giving us hints where plastic flow might occur (fig. 5).

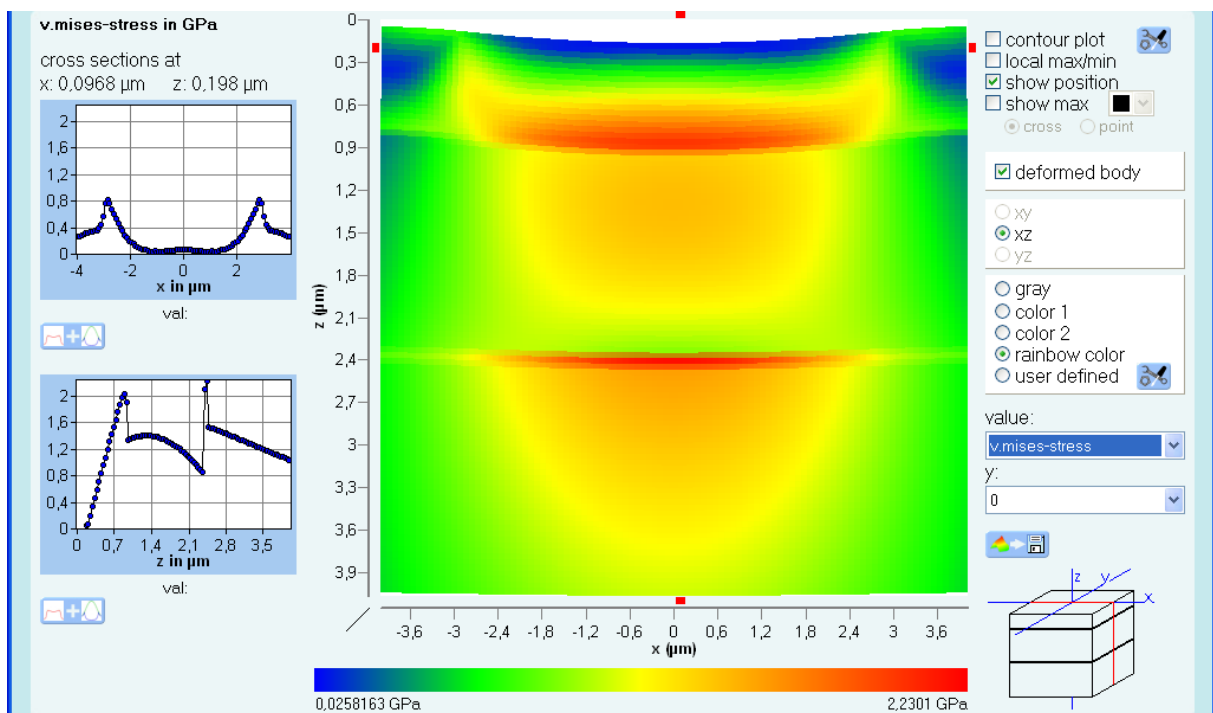


Fig. 5: Resulting von Mises stress distribution around the axis of indentation.

In fact we find two areas in danger at the interfaces to the absorber and the glass substrate (fig. 5). In order to study the stress development of this loading problem more closely, we go back to the load definition page and now chose “fit-load-depth-curve”. There we evaluate a complete penetration-load-curve (fig. 6) for our diamond indenter and let FilmDoctor evaluate the field development during penetration by simply pressing “animate” instead of “calculate” on the calculation page. We perform this evaluation for 10 frames. As there are now

2.800.000 field values to be evaluated the calculation takes about 5 minutes on a small laptop for this 5-layer system.

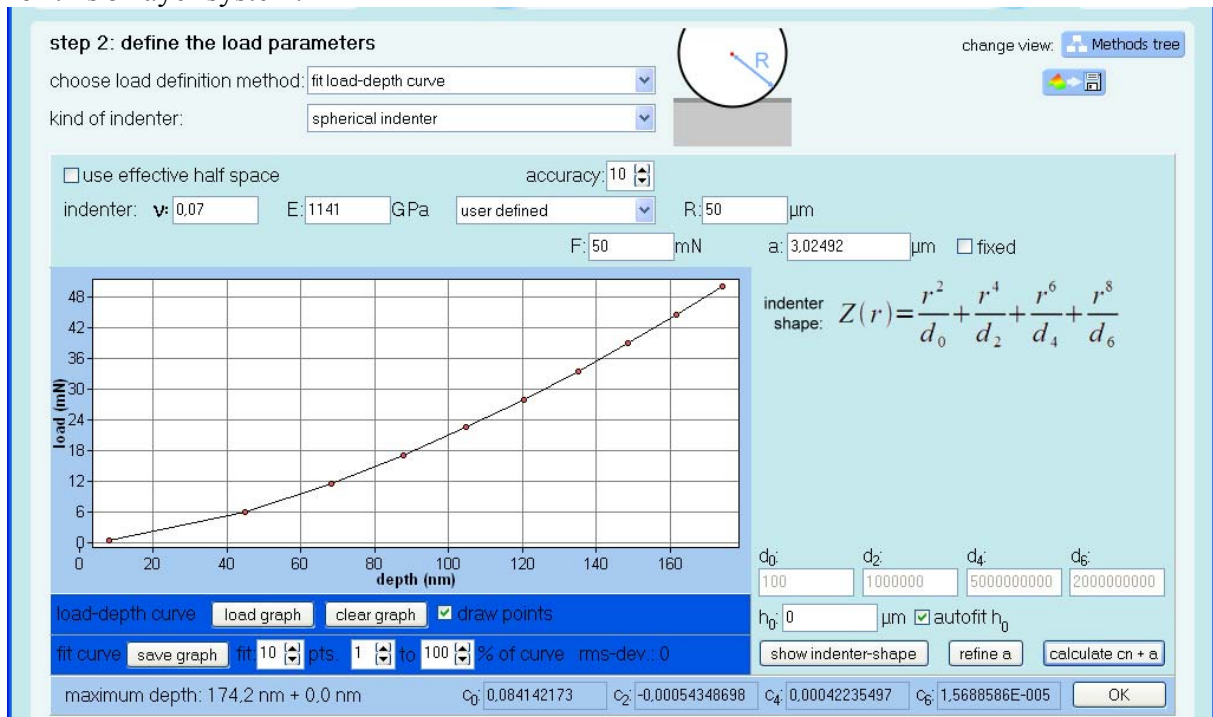


Fig. 6: Load depth curve, evaluated for a 50μm diamond spherical indenter.

This time we look at the radial stress and show only 4 steps of the penetration process (fig. 7).

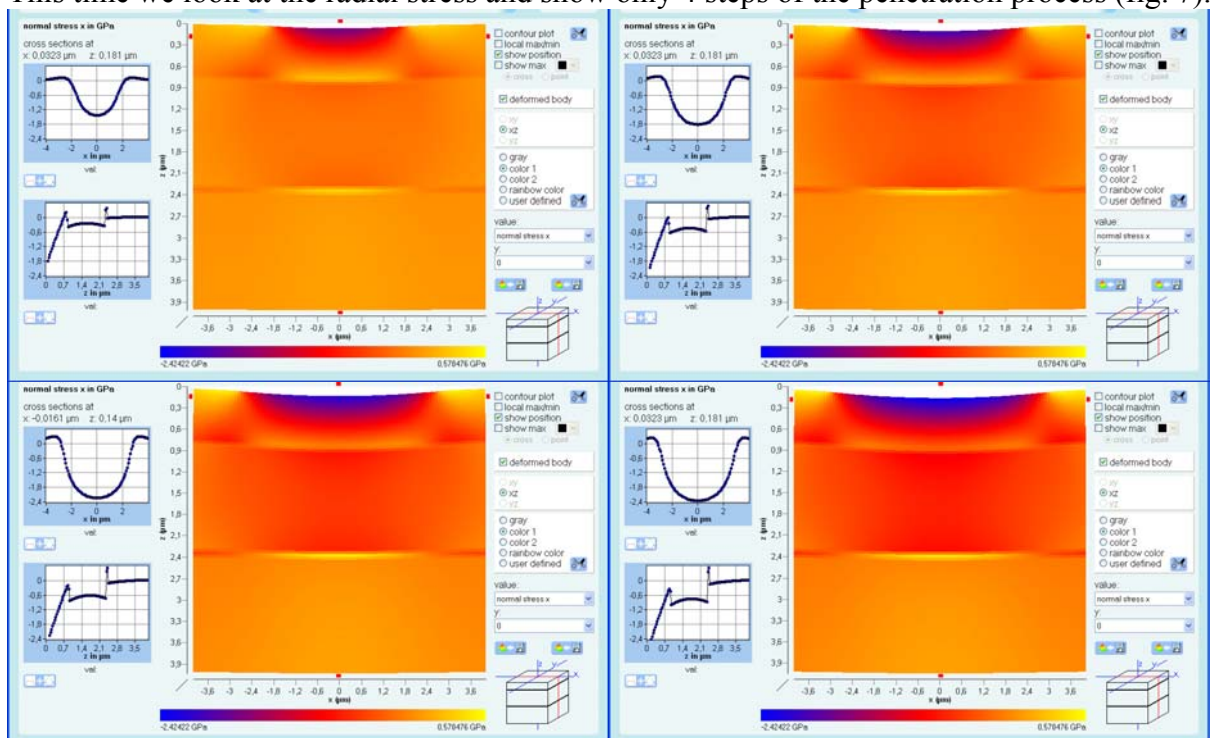


Fig. 7: 2D view of the radial stress development within the plane of indenter axis.

Now we want to simulate scratching effects with small dust particles and reduce the indenter Young's modulus to 150GPa. We also reduce the normal load to 30mN but add now a lateral load component of 20mN simulating the scratching. The stress situation now changes dramatically because instead of having a von Mises maximum somewhere in depth, we now

find strong stress concentrations on the surface for both von Mises and the normal stress in direction of indenter tracking (fig. 8). These stresses lead to fractures on surface.

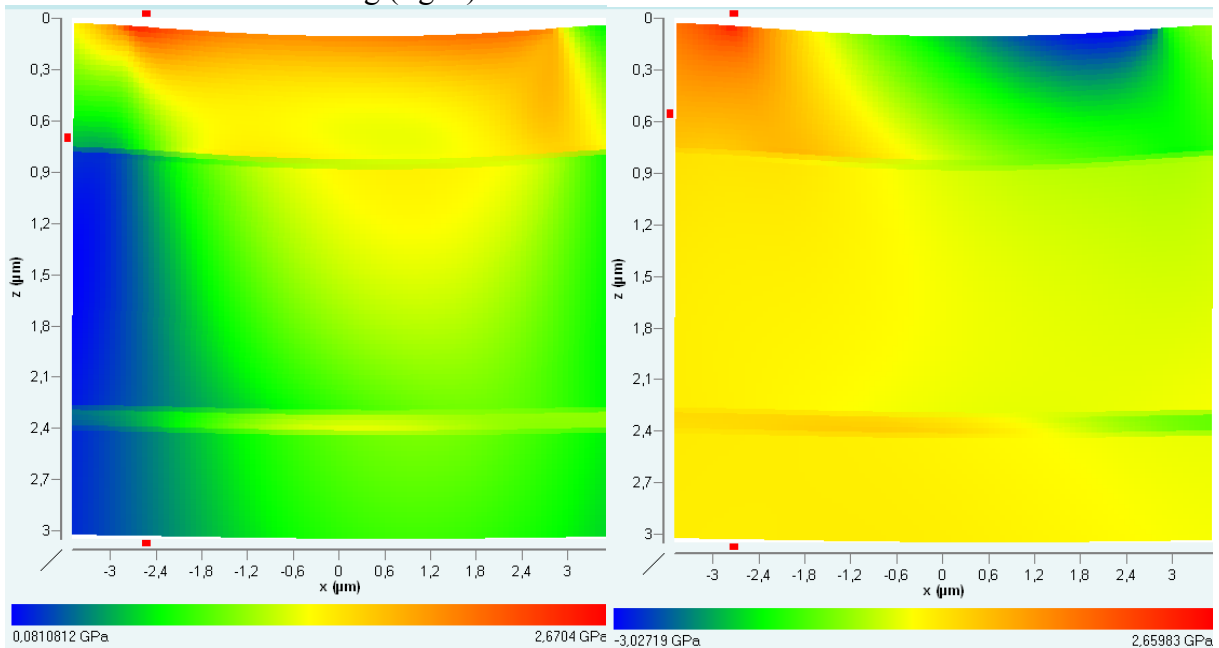


Fig. 8: 2D view of the von Mises (left) and the normal stress (right) in direction of the indenter (simulating the dust particle) track.

Hailstone-Impact

The next example shall show us the effect of an average hailstone with relatively high kinetic energy as they can occur during thunder storms, which will in future increase in number due to the climatic change. With the help of the impact-module in FilmDoctor, we find that a 5mm hailstone with 120km/h would indeed carry a rather threatening kinetic Energy (fig. 9).

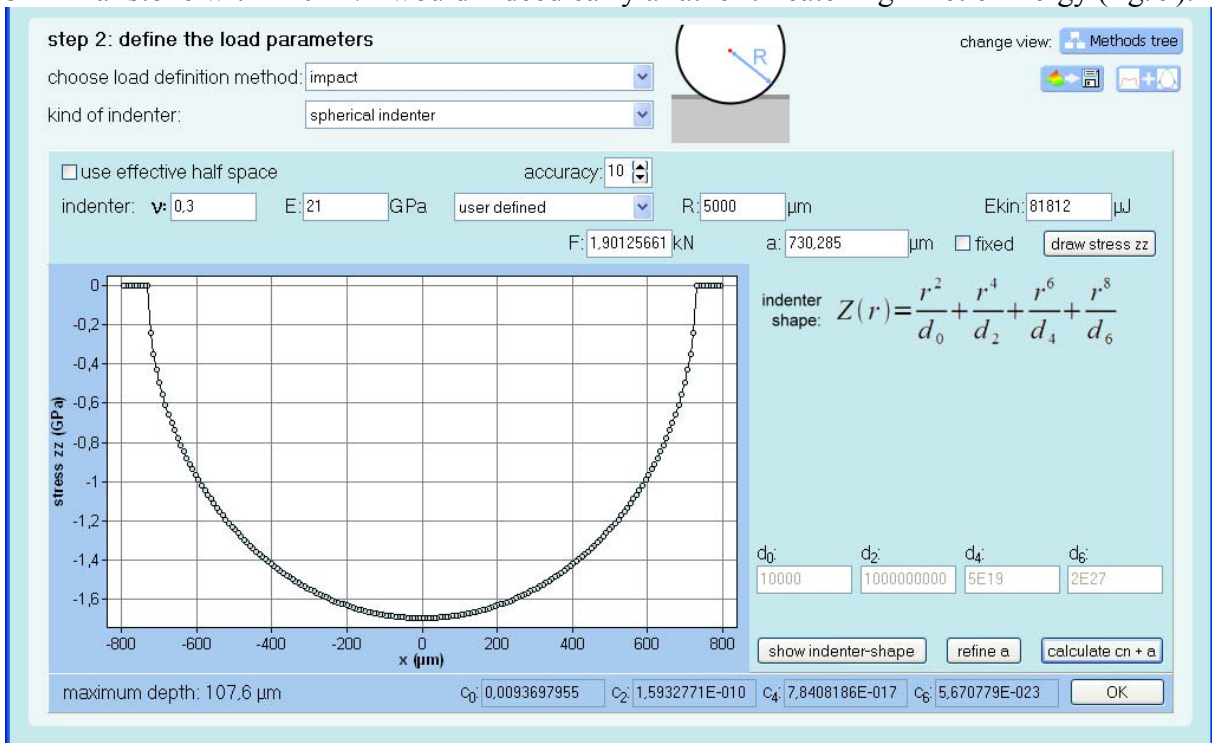


Fig. 9: Resulting normal surface stress for non-inclined impact of a hail stone with 120km/h.

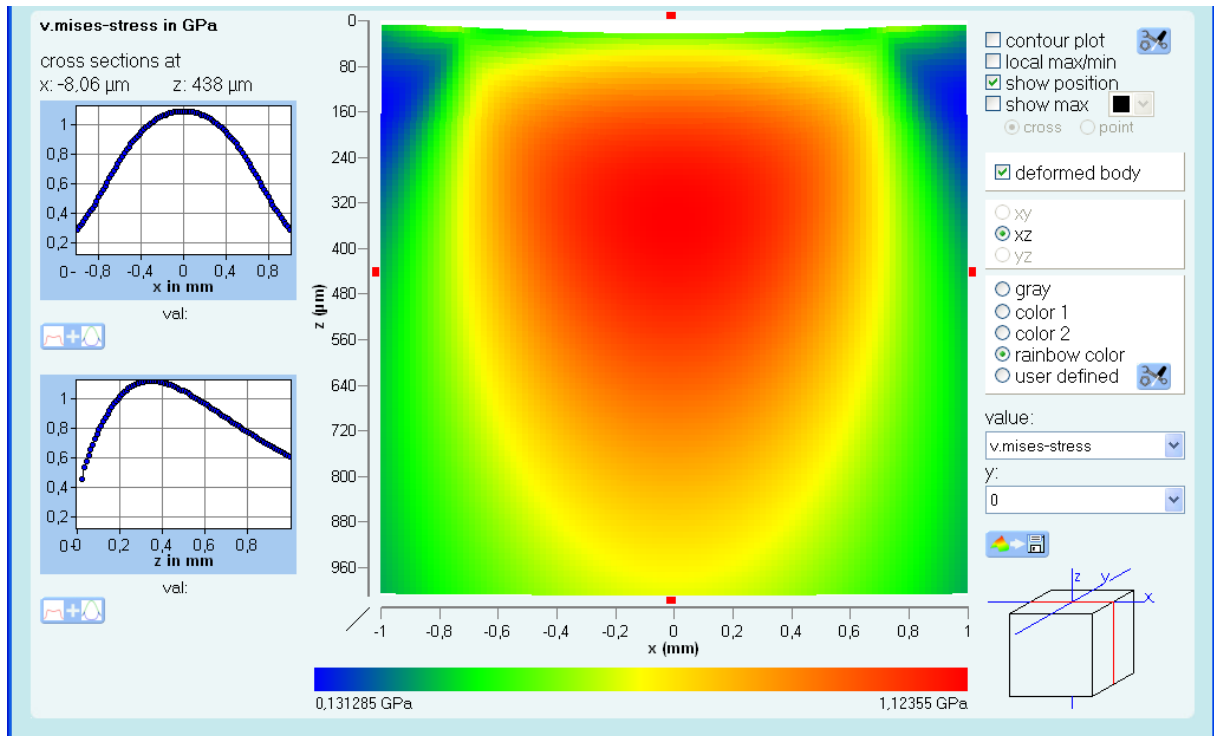


Fig. 10: Resulting von Mises stress shown in the scale of the impacting hailstone.

Nevertheless we find no critical stress distributions if we investigate the impacted area of our thin film solar cell structure in the scale of the impacting hailstone, meaning around 1mm in radial directions and depth (fig. 10). By looking closer at some interfaces however, meaning by zooming out the thin film area, we again find stresses at the buffer and intermediate layers with much too high values. The cell would surely not survive such an impact (fig. 11). Usually, such cell structure are covered with glass plates. Then, one should repeat the evaluation in order to estimate the probability of glass and interface damage possibly leading to additional absorption losses caused by internal defects. Over time such defects can accumulate and yield a sufficient drop in efficiency.

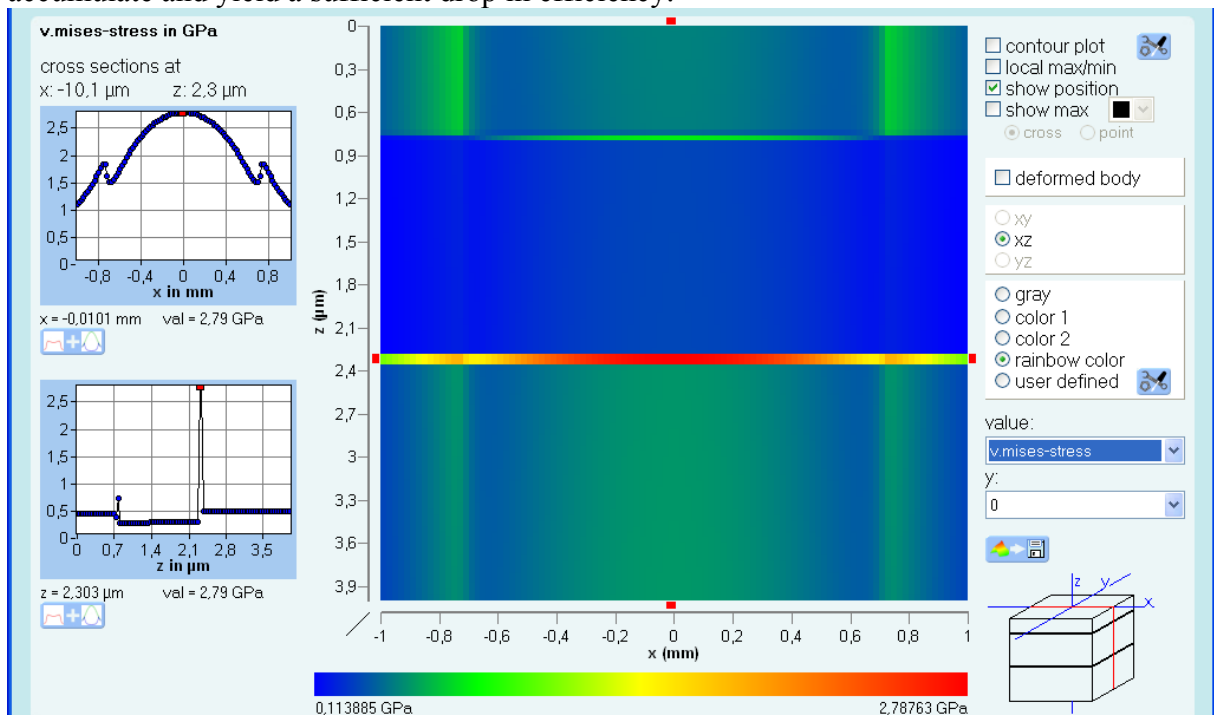


Fig. 11: Resulting von Mises stress shown in the coating scale.

The situation even worsens in the case of inclined impact, especially if a dusty or slightly roughened surface leads to some effective lateral and tilting forces in connection with the impact angle. In this case unbearably high tensile stresses can occur and either destroy the layer structure straight away or lead to initial damage causing failure later (fig. 12 and 13). We should point out here, that we have neglected some aspects of hailstone or droplet impact leading to additional tensile and high shearing stress components (caused by the hailstone or droplet burst), but as already the most simple impact calculation demonstrates us how critical such an impact can be, we have decided to consider such additional effects elsewhere [9].

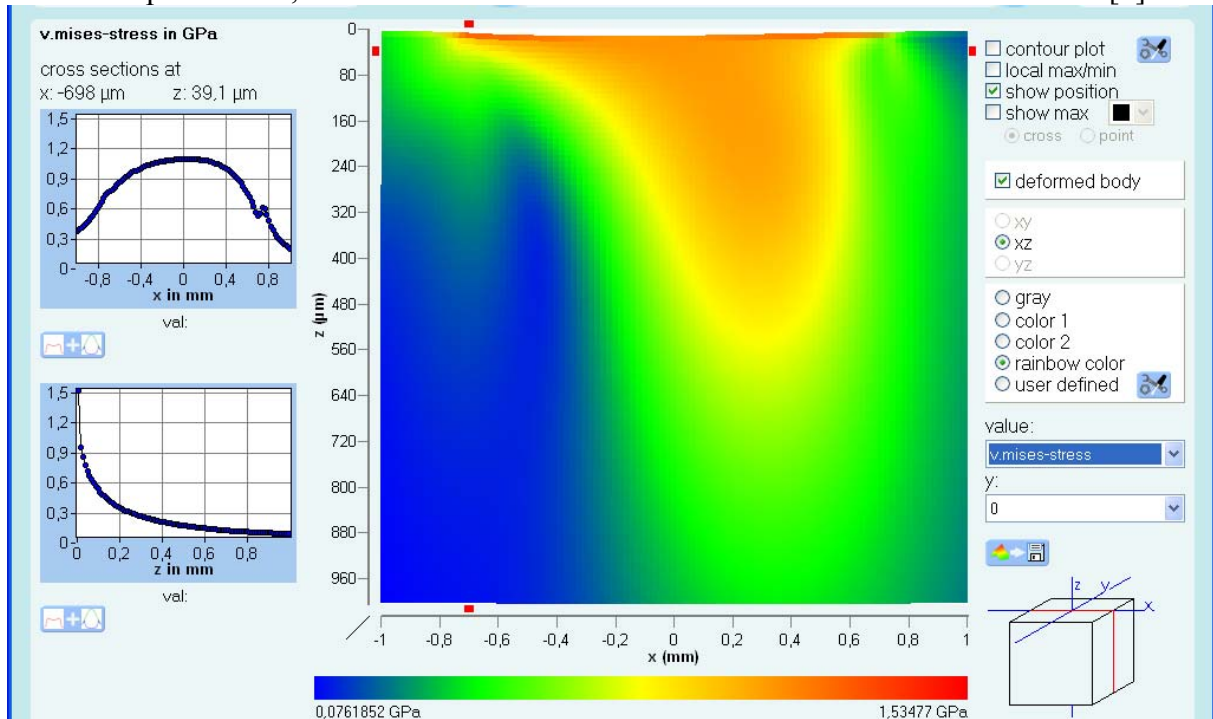


Fig. 12: Resulting von Mises stress shown in the contact scale for the case of an inclined impact situation.

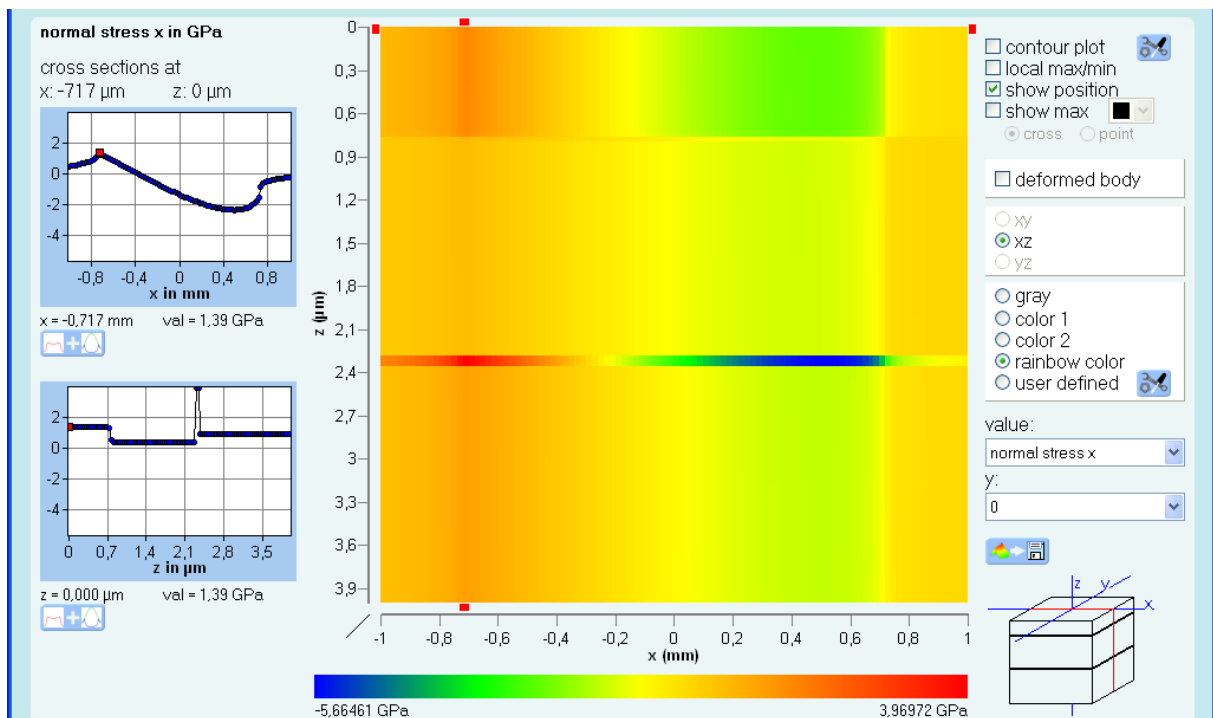


Fig. 13: Resulting radial stress shown in the coating area for the case of an inclined impact situation.

Droplet-Erosion

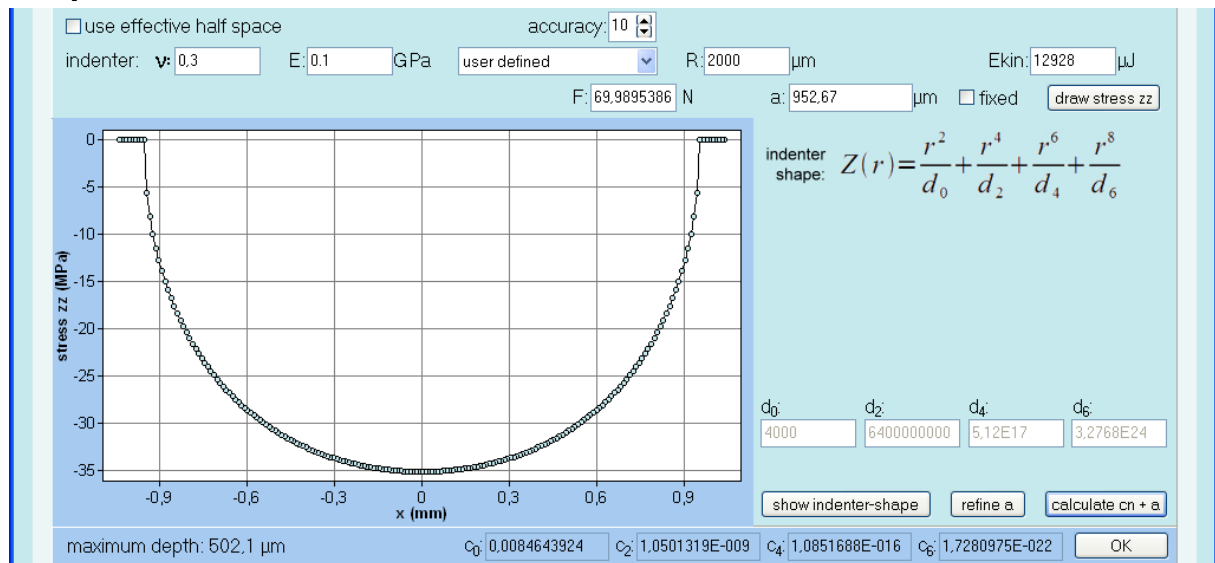


Fig. 14: Resulting normal surface stress for non-inclined impact of a water droplet with 100km/h.

Performing the same impact-evaluation for an ordinary water droplet of 100km/h (fig. 14) results in complete non-critical stress fields during both the impact (fig. 15) and the droplet burst phase (fig. 16).

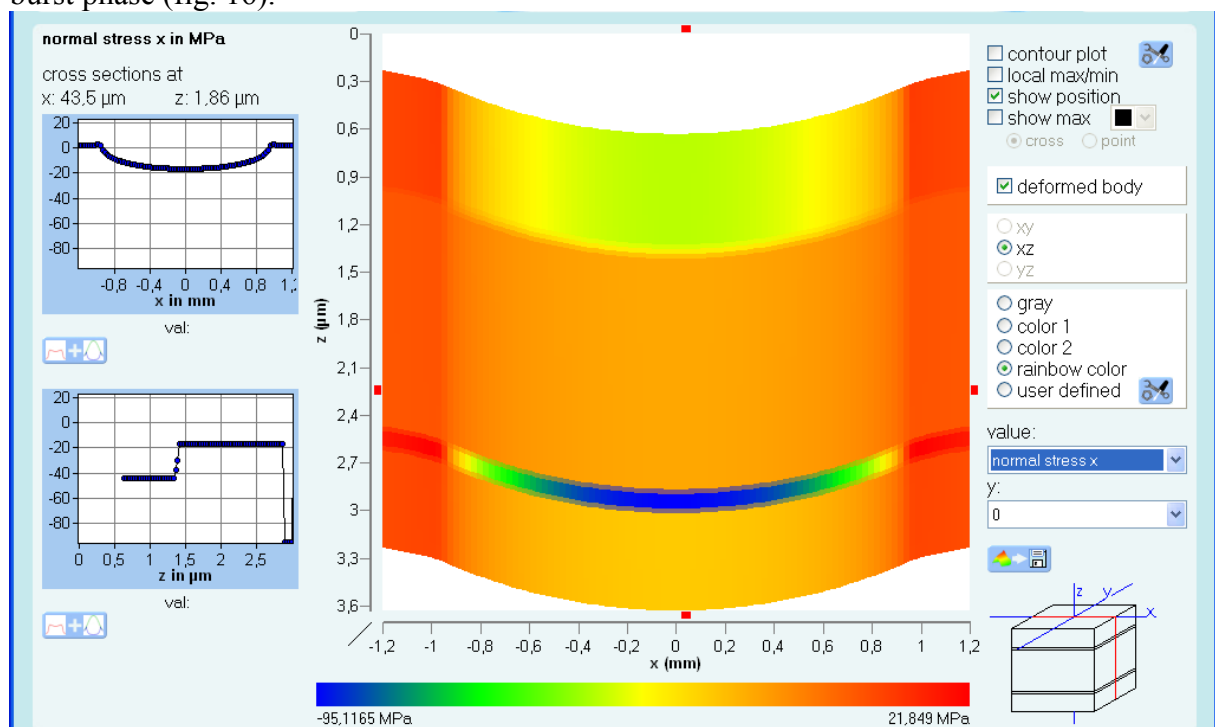


Fig. 15: Resulting normal radial stress for non-inclined impact of a water droplet with 100km/h.

However, it should be pointed out here, that under some conditions so called hot-spots can occur during the burst phase, when very small secondary droplets form and leave the surface producing high “snapping-off” forces (fig. 17).

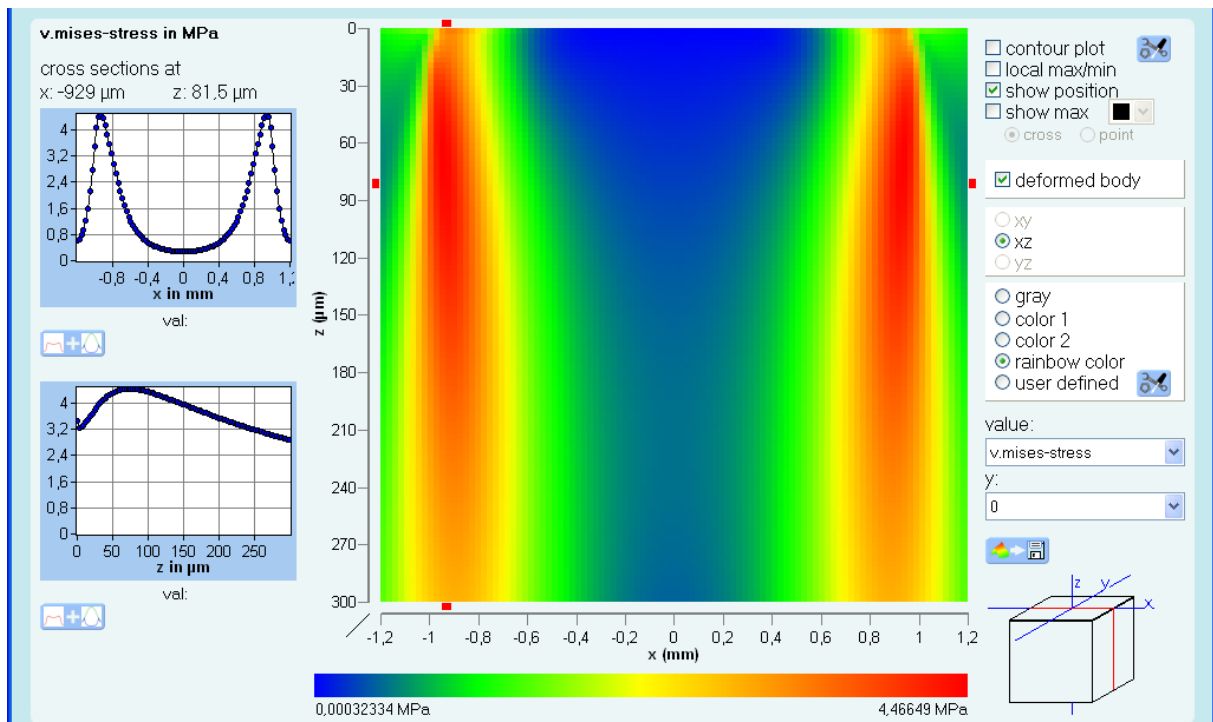


Fig. 16: Resulting von Mises stress for non-inclined impact of a water droplet with 100km/h.

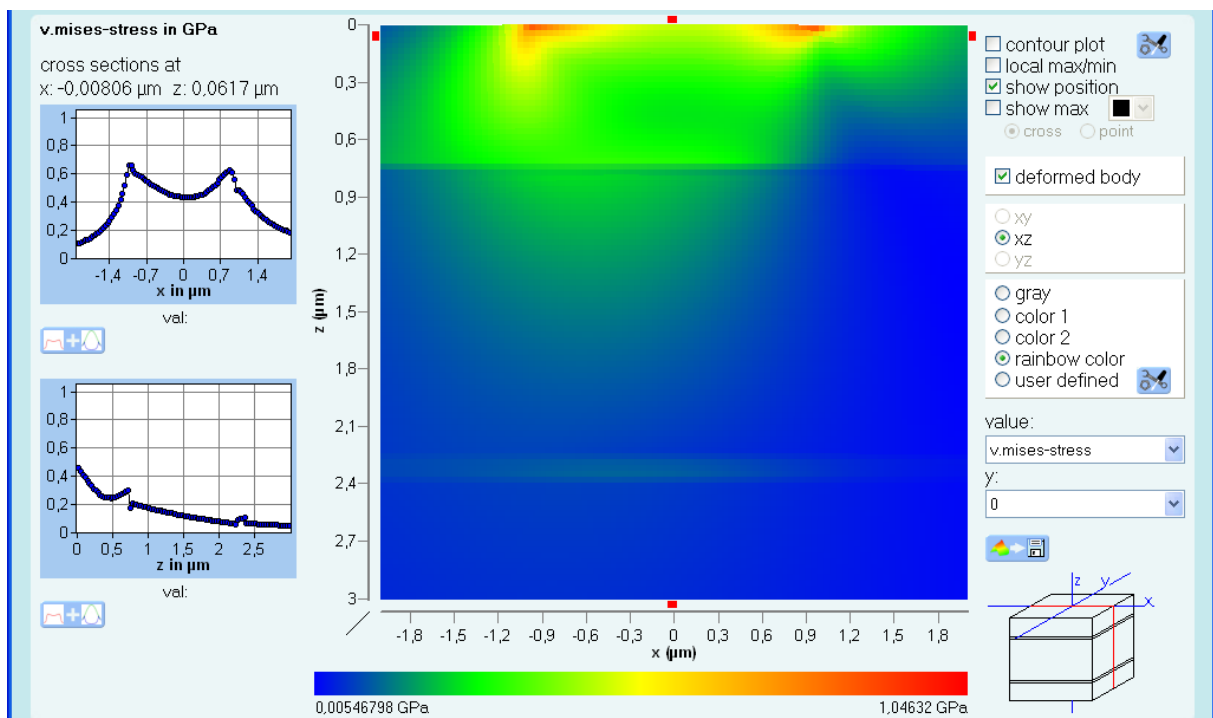


Fig. 17: Resulting von Mises stress of a hot-spot causes by the “snapping-off” of secondary water-droplets.

Internal defects and intrinsic stresses

Another important but still often neglected aspect is that one of intrinsic stresses. Especially in thin film technology intrinsic stresses are almost always part of the layered structures and so they must be taken into account when the external loads possibly occurring during production, transport, installation and service time are simulated. This will be investigated within a more comprehensive study [9].

The same holds for internal defects. Subjected to inevitable external sources of mechanical loads like static wind pressure and oscillations or thermally induced stress fields, the always existing defects and interfaces within the thin film solar cell structures are communicating

with these loads yielding concentrated stress distributions possibly leading to early failure. Figure 18 shows an example evaluation for an interface defect between the ZnO-n- and the ZnO-i-layer.

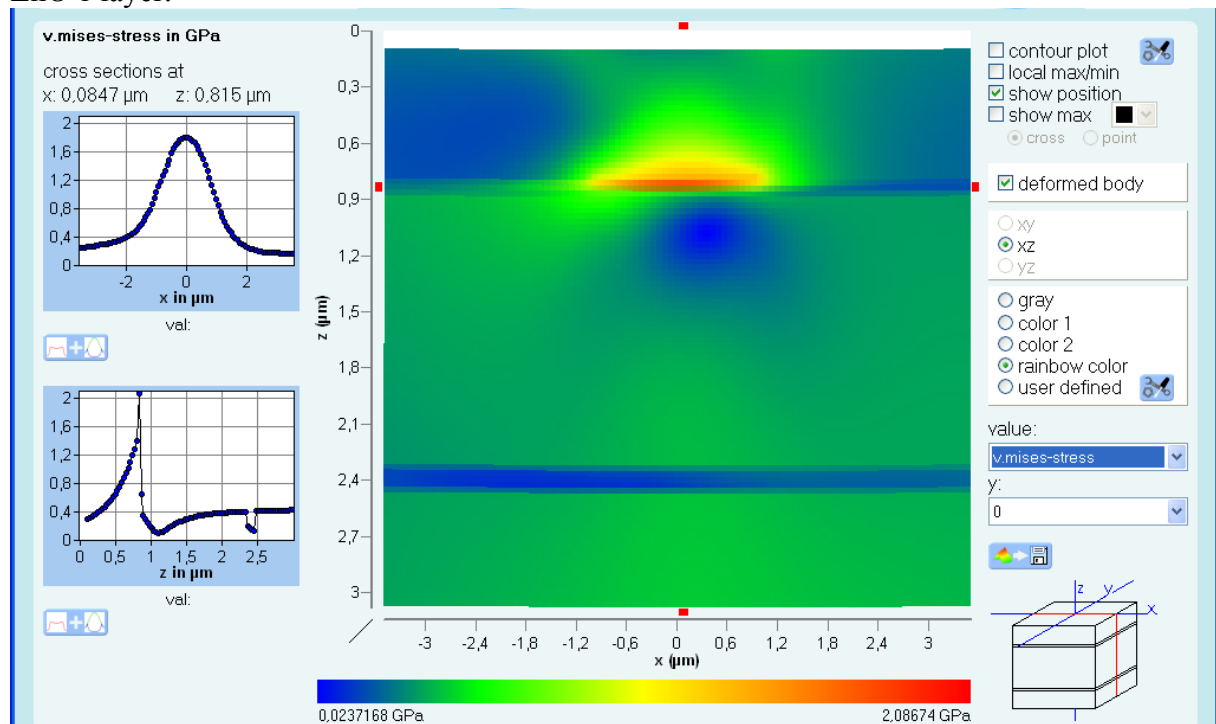


Fig. 18: Resulting von Mises stress of an interface defect “communicating” with a rather small external load.

So even well protected thin film solar cell structures are unavoidably exposed to concentrated stress fields due the communication effect of internal defects and interfaces with external loads and oscillations of the cell and its environment.

Conclusions

It has been demonstrated how by using completely analytical linear elastic modelling methods mechanical loading of thin film solar cell structures can be simulated and investigated under a great variety of conditions. Mechanical loads can lead to concentrated stress distributions yielding material failure, defect accumulation and thus efficiency degradation, because the functionality of the cell is often irrevocably coupled with its mechanical integrity.

As by summing up all mechanical loads the estimated mechanically induced degradation reaches an amount of over 50% of the whole, it might be interesting and worthwhile to consider this wide variety of reasons of failure more closely. This especially holds because many of the concentrated stress fields can be reduced or at least controlled by proper structural, material and protective optimisation holding the degradation-increasing mechanical effects at bay.

References

- [1] Solar Cell Efficiency Tables (Version 27), M. A. Green, K. Emery, D. L. King, Y. Hisikawa, W. Warta, *Progress in Photovoltaics*, **14**, 45-51 (2006)
- [2] N. Schwarzer: “Elastic Surface Deformation due to Indenters with Arbitrary symmetry of revolution”, *J. Phys. D: Appl. Phys.*, **37** (2004) 2761-2772
- [3] N. Schwarzer, G. M. Pharr: „On the evaluation of stresses during nanoindentation with sharp indenters”, proceedings of the ICMCTF 2004 in San Diego, California, USA, also in *Thin Solid Films*, Vol. 469-470C pp. 194-200

- [4] N. Schwarzer, T. Chudoba, G. M. Pharr: „On the evaluation of stresses for coated materials during nanoindentation with sharp indenters”, Surf. Coat. Technol, Vol. 200/14-15 pp 4220-4226
- [5] N. Schwarzer, T. Chudoba, F. Richter: „Investigation of ultra thin coatings using Nanoindentation”, Surface and Coatings Technology, Vol 200/18-19 pp 5566-5580
- [6] N. Schwarzer: "Analysing Nanoindentation Unloading Curves using Pharr's Concept of the Effective Indenter Shape", proceedings of the ICMCTF 2005 in San Diego, California, USA, also in Thin Solid Films 494 (2006) 168 – 172
- [7] N. Schwarzer: "The extended Hertzian theory and its uses in analysing indentation experiments", Phil. Mag. 86(33-35) 21 Nov - 11 Dec 2006 5153 – 5767, Special Issue: “Instrumented Indentation Testing in Materials Research and Development”
- [8] FilmDoctor: software for the evaluation of mechanical loading on monolithic and layered structures, www.siomec.de/filmdoctor
- [9] N. Schwarzer: “About the aspect of intrinsic stresses and defects in connection with mechanically loaded thin film solar cell structures”, to be published